30th Annual International IEEE EMBS Conference
Vancouver, British Columbia, Canada, August 20-24, 2008

# Evaluation of a Neyman-Pearson heart-rate turbulence detector

Juan Pablo Martínez*, Pablo Laguna,
GTC. Aragon Institute of Engineering Research
(I3A) University of Zaragoza / CIBER en
Bioingeniería, Biomateriales y Biomedicina.
{jpmart,laguna}@unizar.es

Kristian Solem, Leif Sörnmo,
Signal Processing Group.
Dept. of Electrical and Information Technology.
Lund University. Sweden.
{kristian.solem,leif.sornmo}@eit.lth.se

*Abstract*— **In this paper we propose and evaluate a Neyman-Pearson approach to detect and characterize heart-rate turbulence after ventricular premature beats (VPB). For quantification of the detection performance an evaluation dataset was built based on real RR interval series. The ROC curves obtained from the test set show the proposed method to outperform the detection capability of the two parameters currently used to quantify turbulence: turbulence onset and turbulence slope.**

*Index Terms*— **Heart rate turbulence, Neyman-Pearson, Karhunen-Loève Transform, detection theory.**

## I. Introduction

Heart rate turbulence (HRT) denotes the typical pattern of the heart rate (HR) subsequent to a ventricular premature beat (VPB). The turbulence consists of an early heart-rate acceleration followed by a deceleration [1]. The mechanisms of this phenomenon are not completely understood, but it is considered as a baroreflex response triggered by the blood pressure drop induced by the VPB. Pharmacological studies have shown that the main role in HRT is played by the parasympathetic branch of the autonomic nervous system [2], though recently a significant correlation between sympathetic burst and HRT parameters has also been found [3].

Heart rate turbulence is currently assessed by two parameters: turbulence onset (TO) and turbulence slope (TS), both obtained from the RR interval series or tachogram following a VPB. Turbulence onset measures the relative change (usually negative) in the RR intervals immediately after the VPB, while turbulence slope quantifies the rate of RR interval increase following the initial heart rate acceleration. Absence of HRT, identified by a non-negative TO or a low TS, has been shown to be a powerful risk predictor in different populations [1].

Recently, a new methodology has been delineated for HRT characterization [4], [5]. There, an extended IPFM (integral pulse modulation model) was proposed, in which the effective modulating signal was the sum of the background HRV and the specific reaction to the VPB (i.e. the possible HRT turbulence). This response was linearly modelled with a Karhunen-Loève transform (KLT) expansion. Based on this model, a statistical detection problem was posed, and a GLRT detector (generalized likelihood ratio test) of the turbulence signal was derived under the white-Gaussian-noise assumption. This detector outperformed the detection ability of TS and TO in simulated signals, and proved to be useful in dialysis patients.

In this work, we assess this concept in a validation dataset constructed from real signals. Similar to [4], [5], we will describe the HRT by using the IPFM modulating signal together with a KLT-based linear model for characterizing the HRT. From the characterization of the RR series according to this model, we explore and evaluate a different approach to discriminate between heart-rate signals with and without turbulence.

## II. Dataset

To assess the detection performance of any HRT measurement, an annotated dataset is needed including a significant number of signals with and without HRT. However, the lack of a gold standard and the low signal-to-noise ratio make it extremely difficult to manually annotate the RR interval series following a single VPB as containing HRT or not. To compensate the absence of annotated databases we created an evaluation dataset with RR interval series obtained from Holter recordings as indicated next.

### A. LTST database.

The Long Term ST database (LTST) [6] contains 68 two-lead and eighteen three-lead 24-hour ambulatory records with significant ST events annotated by medical experts. These records were sampled at 250 Hz with a 12-bit resolution. The database [6]also provides automatic QRS annotations including beat classification supervised by an expert Holter technician.

### B. Dataset construction.

Our approach relies on the assumption that Holter recordings with enough VPBs and a clear HRT pattern measured by TS in the averaged tachogram present an HRT response after every VPB. Thus, RR series around all the VPBs in such records are included in the HRT class ($\mathcal{S}_1$). On the other hand, records with few VPBs or with a blunted HRT in the averaged tachogram were discarded as there is uncertainty about the presence of HRT after the individual VPBs. To overcome this problem, the class of non-HRT series ($\mathcal{S}_0$) was created by including tachograms extracted from periods

*This work was supported by projects TEC-2007-68076-C02-02 from CICYT, and GTC T-30 from DGA (Spain). CIBER de Bioingeniería, Biomateriales y Nanomedicina is an initiative of the ISCIII.

without any premature or ectopic beat, i.e., only containing spontaneous heart rate variability (HRV).

All the VPBs through the 86 records were selected according to the database annotations. Only VPBs preceded by at least 10 normal beats and followed by at least 20 normal beats were considered. VPBs were also discarded if the coupling interval was $\geq 80$ % or the compensatory pause was $< 120$ % of the average RR in the 10 previous beats. After applying those criteria, 64 records remained with suitable VPBs, with only 38 records having more than 15 suitable VPBs. Out of those 38 records, only 26 showed TS $> 2.5$ ms/beat in the averaged tachogram. All the tachograms for the 5764 individual VPBs in those records were included in class $\mathcal{S}_1$. For building class $\mathcal{S}_0$, we extracted 26577 32-beat tachograms from the 10 patients who lacked VPBs. These tachograms provide a characterization of local tachograms without turbulence (or equivalently, a characterization of the background HRV). One hundred tachograms from each class, together with the class averages are shown in Fig. 1.

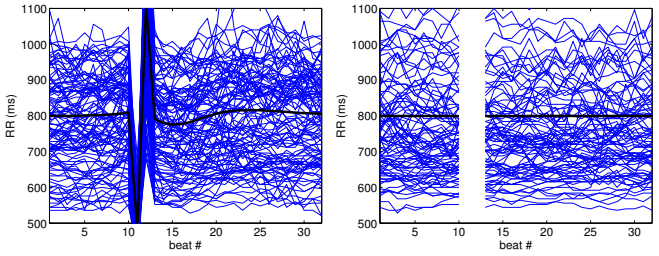


(a) Tachograms in $\mathcal{S}_1$. (b) Tachograms in $\mathcal{S}_0$.

Fig. 1. Tachograms for the HRT ($\mathcal{S}_1$) and non-HRT ($\mathcal{S}_0$) classes. Thick black lines represent the average in the dataset and mean turbulence can be observed in (a). Intervals 11 and 12 correspond to the coupling interval and compensatory pause in (a), and have been blanked in (b) since there are no VPBs in $\mathcal{S}_0$.

## III. METHODS

### A. IPFM extension background

The IPFM model was originally introduced to generate a series of occurence times for sinus beats from a modulating signal $m(t)$ accounting for the autonomic influence on the cardiac pacemaker, reflecting basic electrophysiological properties of the sinoatrial node [7].

Recently, we have proposed an extended IPFM model in order to account for the HRT phenomenon [4], [5]. The extended model includes an additional feedback path which accounts for HRT as an additive signal $s(t)$ triggered by the VPB-induced pressure drop, so that the actual modulating signal of the extended IPFM $x(t)$ is the sum of the background HRV and the feedback signal, i.e., $x(t) = m(t)+s(t)$. The response to the VPB $s(t)$ was modelled as a linear combination of several basis functions, obtained from truncated basis of the KLT. The total modulating signal $x(t)$ after a VPB, which can be estimated from the RR interval series, was considered as an observation of the response to the VPB, considering the background modulating signal as "observation noise".

Thus, the first processing step was to estimate the modulating signal $x(t)$ for each individual tachogram in $\mathcal{S}_0$ and $\mathcal{S}_1$ as described in [4], [5]. Then, the first 10 seconds of the estimated $x(t)$ after each VPB were evenly resampled at 2 Hz to obtain an $N \times 1$ vector $\mathbf{x}$ ($N = 21$). This vector can also be decomposed as the sum of the turbulence and background HRV components: $\mathbf{x} = \mathbf{s} + \mathbf{m}$. The modulating vectors for the example signals in Fig. 1 are plotted in Fig. 2. Note that the shape of the average turbulence (red line) is clearly displayed for class $S_1$.

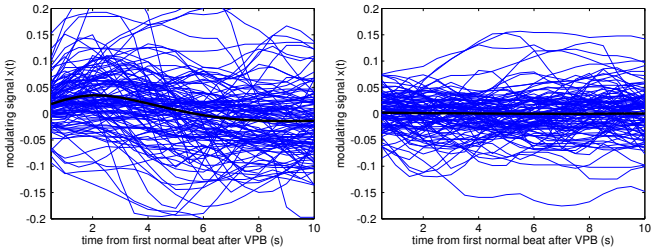


(a) Modulating signals $x(t)$ in $\mathcal{S}_1$. (b) Modulating signals $x(t)$ in $\mathcal{S}_0$.

Fig. 2. IPFM modulating signals after the VPB for the HRT ($\mathcal{S}_1$) and non-HRT ($\mathcal{S}_0$) datasets. Thick black lines represent the average in the dataset.

### B. Signal model for HRT description

In this work, the HRT term for the $l$-th VPB $\mathbf{s}_l$ is modelled as a linear combination of $r$ basis functions

$$\mathbf{s}_l = \mathbf{B}\boldsymbol{\theta}_{\mathbf{s}_l} \tag{1}$$

where $\mathbf{B} = [\mathbf{b}_1, \mathbf{b}_2, \ldots, \mathbf{b}_r]$ contains in its columns the $r$ basis functions and $\boldsymbol{\theta}_{\mathbf{s}_l}$ is the $r \times 1$ coefficient vector associated with the $l$-th VPB. For simplicity, we will drop the VPB index $l$ in the notation in the rest of the paper.

The basis functions $\mathbf{b}_i$ were obtained as the KLT basis for the set of vectors $\mathbf{x}_l$ belonging to the HRT class, $\mathcal{S}_1$. The percentage of the projected energy of each class into the subspace defined by the first $r$ KLT basis functions is shown in Fig. 3(a). Figure 3(b) shows the distribution of the two classes in the first KL coefficients.

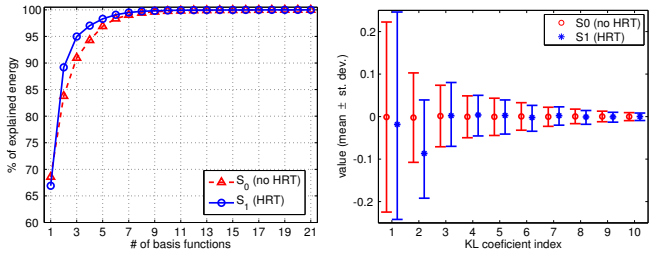


(a) (b)

Fig. 3. (a) Percentage of energy in $S_0$ and $S_1$ explained by the turbulence KLT basis as a function of the basis dimension. (b) Mean $\pm$ 1 standard deviation of the first KL coefficients for vectors in $S_0$ and $S_1$

The three first basis functions (plotted in Fig. 4) account for 95% of the energy in the HRT class. Therefore, we will use $r = 3$ as the linear model dimension.

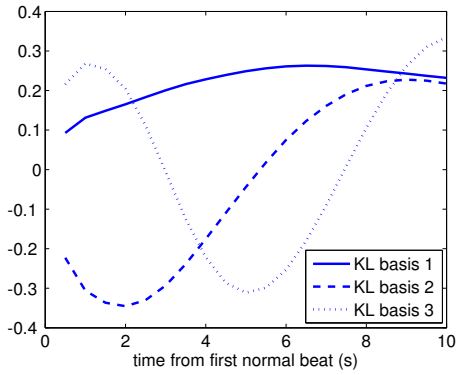


Fig. 4. First three functions of the KLT basis.

We can then formulate a detection problem where HRT is either present (hypothesis $\mathcal{H}_1$) or not (hypothesis $\mathcal{H}_0$) in an observed vector $\mathbf{x}$:

$$\begin{aligned} \mathcal{H}_0: &\quad \mathbf{x} = \mathbf{m} \\ \mathcal{H}_1: &\quad \mathbf{x} = \mathbf{B}\boldsymbol{\theta}_\mathbf{s} + \mathbf{m}. \end{aligned} \tag{2}$$

### C. Statistical methods for HRT detection.

In [4], [5], we used a GLRT detector assuming that $\boldsymbol{\theta}_\mathbf{s}$ is an unknown deterministic vector and $\mathbf{m}$ is a random vector distributed as a white multivariate Gaussian $\mathbf{m} \sim \mathcal{N}(\mathbf{0}, \sigma^2\mathbf{I})$, with $\sigma^2$ unknown. The resulting detection statistic $T(\mathbf{x})$ is proportional to the energy ratio of the projection of $\mathbf{x}$ into the signal subspace (the subspace spanned by $\mathbf{B}$) and its projection to the orthogonal subspace (noise subspace). The underlying assumption is that the background HRV does not project well in the signal subspace and thus, the energy in the signal subspace is higher if HRT is present.

However, Figure 3(a) shows that a 90% of the signal energy in the non-HRT dataset $S_0$ also lies in the first KLT basis functions. Also, the GLRT detector, relying solely on the energy of the projection, is invariant to the sign of the response to the VPB, and therefore does not discriminate physiological turbulences from non-physiological ones.

In this paper, we propose a Neyman-Pearson detector within the reduced signal subspace as an alternative approach for HRT detection. As the three-dimensional subspace defined by the first three KLT basis functions accounts for >90% of the energy in both subsets, we will focus on the coefficients of $\mathbf{x}$ in that reduced subspace: $\theta_\mathbf{x} = \mathbf{B}^T\mathbf{x}$. The detection problem can be now formulated as,

$$\begin{aligned} \mathcal{H}_0: &\quad \boldsymbol{\theta}_\mathbf{x} = \mathbf{B}^T\mathbf{m} = \boldsymbol{\theta}_\mathbf{m} \\ \mathcal{H}_1: &\quad \boldsymbol{\theta}_\mathbf{x} = \boldsymbol{\theta}_\mathbf{s} + \mathbf{B}^T\mathbf{m} = \boldsymbol{\theta}_\mathbf{s} + \boldsymbol{\theta}_\mathbf{m}. \end{aligned} \tag{3}$$

Modelling both the HRT and background HRV components as correlated multivariate Gaussian random vectors with means $\boldsymbol{\mu}$ and $\mathbf{0}$ respectively, we have a detection problem of the form

$$\begin{aligned} \mathcal{H}_0: &\quad \boldsymbol{\theta}_\mathbf{x} \sim \mathcal{N}(\mathbf{0}, \boldsymbol{\Sigma}_0) \\ \mathcal{H}_1: &\quad \boldsymbol{\theta}_\mathbf{x} \sim \mathcal{N}(\boldsymbol{\mu}, \boldsymbol{\Sigma}_1), \end{aligned} \tag{4}$$

where the parameters $\boldsymbol{\mu}, \boldsymbol{\Sigma}_0, \boldsymbol{\Sigma}_1$ can be estimated from a labelled training set. It can be shown [8] that for such a problem, the detection statistic maximizing the probability of detection $P_D$ for a given probability of false alarm $P_{FA}$ (Neyman-Pearson criterion) is given by the likelihood ratio

$$\mathcal{L}(\mathbf{x}) = \frac{p(\mathbf{x};\mathcal{H}_1)}{p(\mathbf{x};\mathcal{H}_0)} = \frac{|\boldsymbol{\Sigma}_0|^{\frac{1}{2}}\exp(-\frac{1}{2}(\boldsymbol{\theta}_\mathbf{x}-\boldsymbol{\mu})^T\boldsymbol{\Sigma}_\mathbf{1}^{-1}(\boldsymbol{\theta}_\mathbf{x}-\boldsymbol{\mu}))}{|\boldsymbol{\Sigma}_1|^{\frac{1}{2}}\exp(-\frac{1}{2}\boldsymbol{\theta}_\mathbf{x}^T\boldsymbol{\Sigma}_\mathbf{0}^{-1}\boldsymbol{\theta}_\mathbf{x})} \tag{5}$$

taking the logarithm and discarding constant terms, we obtain the equivalent detection statistic,

$$\ell(\mathbf{x}) = \boldsymbol{\theta}_\mathbf{x}^T\boldsymbol{\Sigma}_\mathbf{0}^{-1}\boldsymbol{\theta}_\mathbf{x} - (\boldsymbol{\theta}_\mathbf{x}-\boldsymbol{\mu})^T\boldsymbol{\Sigma}_\mathbf{1}^{-1}(\boldsymbol{\theta}_\mathbf{x}-\boldsymbol{\mu}). \tag{6}$$

It must be noted that $\Sigma_0$ and $\Sigma_1$ are not explicitly related to each other in equations (4) and (6), and therefore the model, and, consequently, the detection statistic (6) are general and do not assume additivity of HRT and HRV.

### D. Evaluation

To evaluate the proposed approach as well as the parameters TO and TS, each of the two classes: $\mathcal{S}_0$ and $\mathcal{S}_1$, was divided in two halves: the first half ($\mathcal{S}_{0ts}$ and $\mathcal{S}_{1ts}$) was used as test set while the second half ($\mathcal{S}_{0tr}$ and $\mathcal{S}_{1tr}$) was used as training set to estimate the model parameters.

## IV. HRT Detection Results

The parameters $\boldsymbol{\mu}, \boldsymbol{\Sigma}_0, \boldsymbol{\Sigma}_1$ were estimated as the sample mean vector and sample covariance matrices of vectors $\boldsymbol{\theta}_\mathbf{x} = \mathbf{B}^T\mathbf{x}$ in datasets $\mathcal{S}_{0tr}$ and $\mathcal{S}_{1tr}$.

Figure 5(a) shows the scatterplot of the vectors $\mathbf{x} \in \mathcal{S}_0, \mathcal{S}_1$ in the subspace defined by the first 3 KL basis functions. Each point represents the RR interval series after a single VPB. A wide overlap can be observed between the two datasets. Note that the detection statistic (6) provides a quadratic separation surface between the two groups. Figure 5(b) shows the ROC curves of the proposed detector, as well as the TO and TS parameters in the test set.

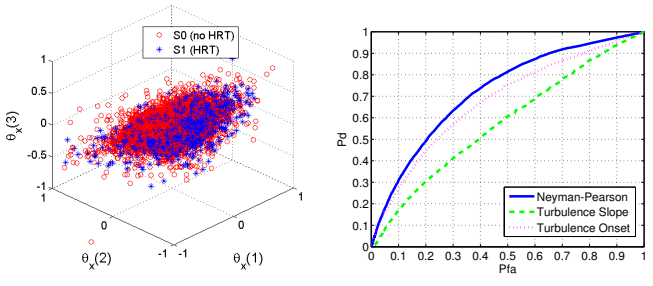


(a) (b)

Fig. 5. (a) Scatterplot of $\theta_\mathbf{x}$ and (b) ROC curves for statistic $\ell(n)$, TO and TS for individual VPBs in the test set.

Figures 6(a) and 7(a) show that the groups become more separable when the series for 10 or 100 consecutive VPBs are averaged, as it is usually done in HRT analysis. The ROC curves for averaged series are shown in Fig. 6(b) and 7(b). Note that the model parameters have not been reestimated for averaged series (i.e., the parameters in (6) were computed using the series for individual VPBs in the training set).

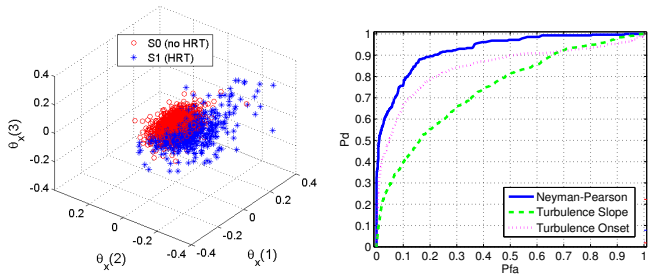


(a) (b)

Fig. 6. (a) Scatterplot of $\theta_{\mathbf{x}}$ and (b) ROC curves for statistic $\ell(n)$, TO and TS for averages of 10 VPBs in the test set.

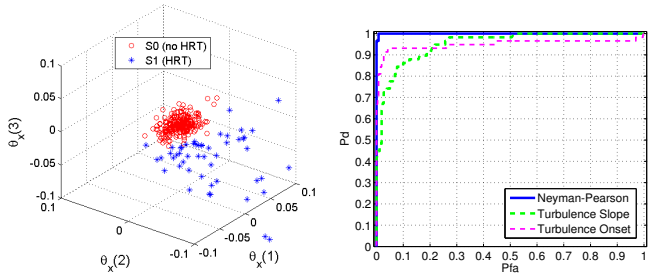


(a) (b)

Fig. 7. (a) Scatterplot of $\theta_{\mathbf{x}}$ and (b) ROC curves for statistic $\ell(n)$, TO and TS for averages of 100 VPBs in the dataset.

## V. Discussion and conclusion

### A. Models and methods.

In this paper, we have proposed and evaluated a new methodology for HRT characterization. The method is based on the representation of the IPFM modulating signal after a VPB in the subspaced defined by the most relevant KLT basis functions for signals with HRT.

To characterize the HR signals when HRT is present and when it is absent, we have created a labelled dataset of RR interval series from real Holter ECG signals as described in Section II, thus circumventing the need for simulation.

Figure 3 shows that the background HRV, which can be understood as the noise term in the model of eq. (2), is also quite well represented in the *signal subspace*. Due to this overlap, a subspace energy detector is suboptimal.

Therefore, we have focused on the signal subspace (as a good representation for both groups of signals) and have designed a Neyman-Pearson detector modelling both datasets as multivariate Gaussian with general and possibly different covariance matrices (eq. (4)). Note that the signal model (4) assumed this work is quite general and may be valid even if the interaction between background HRV and HRT is not additive.

### B. HRT detection performance.

For individual VPBs, fixing $P_{FA} = 0.1$ (10% of abnormal series, i.e., series without turbulence, would be considered as normal), the $P_D$ is 0.3 for the proposed detector, 0.25 for TO and 0.15 for TS. When averaging 10 consecutive VPBs, $P_D$ attains 0.76, 0.66 and 0.4 respectively for the same $P_{FA}$. If 100 VPBs are available, the Neyman-Pearson detector outperforms TO and TS, obtaining almost perfect discrimination.

Therefore it can be concluded that the proposed model-based detector can discriminate between series with and without HRT better than the commonly used TO and TS parameters, making possible the analysis of HRT with a reduced number of VPBs. This results encourage further evaluation in clinical datasets to determine whether this performance improvement results in better prediction of cardiac risk.

## References

[1] G. Schmidt, M. Malik, P. Barthel, R. Schenider, K. Ulm, L. Rolnitzky, A. J. Camm, J. T. Bigger, and A. Schömig, "Heart-rate turbulence after ventricular premature beats as a predictor of mortality after acute myocardial infarction," *Lancet*, vol. 353, pp. 1390–1396, 1999.

[2] D. Wichterle, V. Melenovsky, J. Simek, J. Malik, and M. Malik, "Hemodynamics and autonomic control of heart rate turbulence," *Journal of Cardiovascular Electrophysiology*, vol. 17, no. 3, pp. 286–291, 2006.

[3] N. M. Segerson, S. L. Wasmund, M. Abedin, R. K. Pai, M. Daccarett, N. Akoum, T. S. Wall, R. C. Klein, R. A. Freedman, and M. Hamdan, "Heart rate turbulence parameters correlate with post-premature ventricular contraction changes in muscle sympathetic activity," *Heart Rhythm*, vol. 4, no. 3, pp. 284–289, 2007.

[4] K. Solem, P. Laguna, J. P. Martínez, and L. Sörnmo, "Performance evaluation of heart rate turbulence detection using an extended ipfm model," in *Computers in Cardiology*, vol. 34, 2007, pp. 821–824.

[5] ——, "Model based detection of heart rate turbulence," *IEEE Trans. on Biomed. Eng.*, vol. (In Press), 2008.

[6] F. Jager, A. Taddei, G. B. Moody, M. Emdin, G. Antolic, R. Dorn, A. Smrdel, C. Marchesi, and R. G. Mark, "Long-term ST database: a reference for the development and evaluation of automated ischaemia detectors and for the study of the dynamics of myocardial ischaemia," *Med. Biol. Eng. Comp.*, vol. 41, no. 2, pp. 172–183, 2003.

[7] L. Sörnmo and P. Laguna, *Biomedical Signal Processing in Cardiac and Neurological Applications*. Elsevier Academic Press, London, 2005.

[8] S. M. Kay, *Fundamentals of Statistical Signal Processing. Detection theory*. Upper Saddle River: Prentice Hall, 1993.